Effects of Future Climate and Biogenic Emissions Changes on Surface Ozone over the United States and China

JIN-TAI LIN AND KENNETH O. PATTEN

Department of Atmospheric Sciences, University of Illinois at Urbana–Champaign, Urbana, Illinois

KATHARINE HAYHOE

Department of Atmospheric Sciences, University of Illinois at Urbana–Champaign, Urbana, Illinois, and Department of Geosciences, Texas Tech University, Lubbock, Texas

XIN-ZHONG LIANG

Illinois State Water Survey, University of Illinois at Urbana–Champaign, Urbana, Illinois

DONALD J. WUEBBLES

Department of Atmospheric Sciences, University of Illinois at Urbana–Champaign, Urbana, Illinois

(Manuscript received 2 January 2007, in final form 10 December 2007)

ABSTRACT

Future projections of near-surface ozone concentrations depend on the climate/emissions scenario used to drive future simulations, the direct effects of the changing climate on the atmosphere, and the indirect effects of changing temperatures and CO_2 levels on biogenic ozone precursor emissions. The authors investigate the influence of these factors on potential future changes in summertime daily 8-h maximum ozone over the United States and China by comparing Model for Ozone and Related Chemical Tracers, version 2.4, (MOZART-2.4) simulations for the period 1996–2000 with 2095–99, using climate projections from NCAR–Department of Energy Parallel Climate Model simulations driven by the Intergovernmental Panel on Climate Change Special Report on Emissions Scenarios A1fi (higher) and B1 (lower) emission scenarios, with corresponding changes in biogenic emissions. The effect of projected climate changes alone on surface ozone is generally less than 3 ppb over most regions. Regional ozone increases and decreases are driven mainly by local warming and marine air dilution enhancement, respectively. Changes are approximately the same magnitude under both scenarios, although spatial patterns of responses differ. Projected increases in isoprene emissions (32%–94% over both countries), however, result in significantly greater changes in surface ozone. Increases of 1–15 ppb are found under A1fi and of 0–7 ppb are found under B1. These increases not only raise the frequency of "high ozone days," but are also projected to occur nearly uniformly across the distribution of daily ozone maxima. Thus, projected future ozone changes appear to be more sensitive to changes in biogenic emissions than to direct climate changes, and the spatial patterns and magnitude of future ozone changes depend strongly on the future emissions scenarios used.

1. Introduction

Regional ozone concentrations are likely to be affected by changes in future climate and biogenic emissions in the coming decades (Denman et al. 2007), as illustrated by numerical simulations with both global (Racherla and Adams 2006; Murazaki and Hess 2006, hereinafter MH06) and regional (Tao et al. 2003, 2007; Hogrefe et al. 2004; Kunkel et al. 2008) models. Using the Community Multiscale Air Quality (CMAQ) modeling system, for example, under the Intergovernmental Panel on Climate Change (IPCC) Special Report on Emission Scenarios (SRES) A2 mid–high emissions scenario, Hogrefe et al. (2004) found that U.S. ozone would increase 1.5–7.5 ppb by the 2080s over the Northeast and Midwest because of climate change together with the resulting changes in biogenic emissions. Using

Corresponding author address: Donald J. Wuebbles, Department of Atmospheric Sciences, University of Illinois at Urbana–Champaign, 105 S. Gregory St., Urbana, IL 61801.
E-mail: wuebbles@atmos.uiuc.edu

DOI: 10.1175/2007JAMC1681.1

a global model driven by the midrange A1b scenario, MH06 found that summertime surface daily 8-h maximum (D8hM) ozone concentrations would increase up to 4 ppb by the 2090s over much of the inland eastern United States in response to future climate change (without considering changes in biogenic emissions). Tao et al. (2007) conducted a suite of 1-yr simulations with the Air Quality Model (AQM) to investigate the relative contributions of projected climate changes and precursor emissions changes to the changes in summertime D8hM ozone over the United States from 1998 to 2050. They found that projected U.S. ozone changes are primarily determined by anthropogenic precursor emissions changes under the higher A1fi scenario, but by changes in climate and biogenic precursor emissions under the lower B1 scenario. Also, through AQM simulations for 1996–2000 and 2095–99, Kunkel et al. (2008) estimated future changes in summertime D8hM ozone concentrations over the Northeast and found that, depending on the cumulus scheme used, the D8hM ozone could increase by 10%–30% because of changes in both climate and biogenic emissions under the A1fi scenario but decrease by 1%–13% under the B1 scenario.

One of the primary barriers to simulating future surface ozone is the uncertainty in projections of changes in response to future climate and biogenic emissions. Increases in global average surface air temperature and associated climatic changes depend on the assumptions made regarding future population growth, technological development, energy sources, and other factors driving human emissions over the coming century. At the higher end of the range, a continued reliance on fossil fuels is estimated to produce atmospheric carbon dioxide (CO_2) concentrations greater than 950 ppm by the end of the century under the higher A1fi scenario. At the lower end, an emphasis on sustainability and conservation results in atmospheric CO_2 concentrations reaching only ~550 ppm by the end of the century under the lower B1 scenario (Prentice et al. 2001). The best estimate for global temperature change from 1980–99 to 2090–99 under the A1fi scenario is 4.0 K, with a range of 2.4–6.4 K, depending on the sensitivity of the climate system to increased emissions of greenhouse gases (Meehl et al. 2007). Under B1, by comparison, global temperatures are projected to increase by 1.1 to 2.9 K, with a best estimate of 1.8 K, from 1980–99 to 2090–99.

Estimation of present-day biogenic ozone precursor emissions is already uncertain. Factoring in their temperature dependence and the actual change that would be induced by this range of future temperature change adds an additional layer of uncertainty that causes climate-induced changes in biogenic emissions to vary substantially over the range of future scenarios. As a result, the projected effects of climate and biogenic emissions on surface ozone over the coming century, including the individual roles played by climate changes and biogenic emissions changes, may vary substantially, depending on the scenario assumed. However, with the exception of Tao et al. (2007) and Kunkel et al. (2008), previous studies generally examined changes under one future scenario only. Thus, they were not able to investigate the potential range of future ozone response to climate and biogenic emissions changes (e.g., Hogrefe et al. 2004; Racherla and Adams 2006; MH06). Moreover, MH06 did not include the changes in biogenic emissions. The motivation for this study is therefore to simultaneously examine projected changes in surface ozone due to the combined and individual effects of future climate and biogenic emissions in order to identify the range in potential changes that would be projected to occur under higher as compared to lower future climate–emission scenarios.

Since all the scenarios used by previous studies, such as the SRES mid–high A2 (Hogrefe et al. 2004; Racherla and Adams 2006) and midrange A1b (MH06), lie within the range bounded by A1fi and B1, the uncertainty in projections of climate-related ozone change in future years can be roughly inferred by the differences in ozone changes between A1fi and B1. Although future climate change could end up being either greater than A1fi or smaller than B1, depending on the policy choices being made currently and over the next few decades, the range of climate change bounded by A1fi and B1 encompasses the current uncertainty in "business as usual" futures, at least in terms of greenhouse gas emissions and the resulting climate change.

It is important to note, however, that each scenario also contains different assumptions regarding ozone precursor emissions from anthropogenic sources, which are not necessarily bounded by A1fi and B1; hence, the resulting ozone projections from the combined effects of climate change and anthropogenic ozone precursor emissions changes may also be dependent on the specific scenario rather than bounded by A1fi and B1. The effects of anthropogenic precursor emissions projections on ozone concentrations are not considered in the present study. Furthermore, the climate simulations used here are from the National Center for Atmospheric Research (NCAR)–U.S. Department of Energy (DOE) Parallel Climate Model (PCM), which has a climate sensitivity value (climate sensitivity being a measure of the magnitude of the response of global surface temperature to increases in greenhouse gas concentrations) at the lowest end of the currently accepted range. The projections of climate change used here

therefore represent the lower end of what would be expected under a given scenario, as the climate changes simulated by other general circulation models for the same emissions scenarios are proportionally greater.

Regional model simulations by Tao et al. (2007) and Kunkel et al. (2008) have used both the A1fi and the B1 scenarios to examine surface ozone responses to climate and biogenic emissions projections. While both studies provided an insightful investigation of future ozone projections due to climate and biogenic emissions changes, they were limited by their simplified treatment of lateral boundary conditions (LBCs) for chemical concentrations. In both studies, the same time-invariant vertical profiles of ozone and other gaseous species were used as the chemical LBCs for both current and future periods; thus, the effects of changes in long-range transport could not be accounted for. Hogrefe et al. (2004) and Steiner et al. (2006) found that projected changes in chemical LBCs were one major factor of future pollutant changes over the eastern United States and California, respectively, in their regional model simulations. In particular, in the analysis of Hogrefe et al. (2004), the largest contributor of projected changes in summer average D8hM ozone concentrations from the 1990s to the 2050s was identified as a simple alteration of chemical LBCs according to projected changes in global tropospheric column concentrations (for ozone) and surface emissions for the Organization for Economic Cooperation and Development as of 1990 (OECD90) region [for nitrogen oxides (NO_x) and volatile organic compounds (VOCs)], followed by changes in regional climate and anthropogenic emissions. In addition, Tao et al. (2007) only conducted single-year simulations and thus were not able to project a climatological change in U.S. ozone, while Kunkel et al. (2008) did not separate the effects of climate change from the effects of biogenic emissions changes. Therefore, in this study, we use the global chemical transport model (CTM), Model for Ozone and Related Chemical Tracers, version 2.4, (MOZART-2.4) to project climatological changes in surface ozone over the coming century in response to the combined and separate effects of climate changes and biogenic emissions changes. These results are designed to be used in further regional modeling studies, as these time-dependent global CTM results can then be used as the chemical LBCs for regional models such as those used in Tao et al. (2007) and Kunkel et al. (2008).

To examine the potential effects of higher versus lower emissions on surface ozone changes over the coming century, we focus on two very different nations: the United States and China (particularly the eastern half, east of 105°E, because of its concentrated population). Although halfway across the world from each other, the two countries are located at similar latitudes and share some common aspects influencing their ozone air quality. For example, solar radiation and surface air temperature both peak during the summer (June–August) period in both countries. Also, relatively large population centers and anthropogenic precursor emissions are located over coastal areas. However, the seasonal characteristics of ozone pollution do differ significantly between the two countries because of the differences in the large-scale atmospheric circulation patterns. In the United States, surface ozone concentrations are typically at their maximum in summer because of strong solar radiation, high air temperature, and strong anthropogenic and biogenic precursor emissions, which result in effective ozone production. In eastern China, in contrast, ozone concentrations in summer are usually lower than in spring and autumn because of strong dilution effects of marine air masses brought in by the prevailing Asian summer monsoon (Mauzerall et al. 2000; Wang et al. 2006 and references therein; Pochanart et al. 2002). In addition, biogenic emissions differ greatly between the two countries because of their distinctive vegetation coverage (Tie et al. 2006). Over the United States, there is significant amount of vegetation over most of the eastern half of the country with maximum vegetation-related emissions in the Southeast, especially in summer. In contrast, there is little vegetation coverage over much of the northern part of eastern China (from 30° to 40°N) because of its high population density. Because of both the similarities and the differences in the factors controlling summer surface ozone over the United States and China, it is therefore interesting to compare projected changes in climate and biogenic emissions and their effects on ozone levels between the two countries. It is particularly important to examine the potential changes in marine air influence on ozone over the coastal areas of both countries.

To identify the relative effects of emission scenarios, climate change, and biogenic emissions, we examine projected future summer (June–August) surface ozone changes over the United States and China from the present day (1996–2000) to the late twenty-first century (2095–99). Changes are projected to occur in response to projected changes in climate and changes in biogenic precursor emissions, together and separately, under the A1fi and B1 scenarios. In this study, anthropogenic precursor emissions are kept unchanged at present-day levels. All simulations are conducted continuously for each five-year period, but our analyses are focused on the June–August summer period, when the difference in surface ozone concentrations over the United States

and China is at its maximum as a result of their differences in the large-scale circulation. Moreover, the effects of changes in climate (e.g., air temperature, marine air influence) and biogenic emissions on surface ozone levels over the two countries are most significant in the summer months.

2. Model and methods

MOZART-2.4 [described and evaluated in detail by Horowitz et al. (2003)] is a state-of-the-art global CTM commonly used to study tropospheric distributions and changes of ozone and related tracers (e.g., Wuebbles et al. 2001; Wei et al. 2002; Horowitz et al. 2003; Lamarque et al. 2005; MH06; Lin et al. 2008). The model simulates 63 species, 135 gaseous reactions, and 26 heterogeneous processes. The advection, surface emission–deposition, vertical diffusion, convection, cloud–precipitation, and chemistry are integrated in order at every time step. Following MH06 and Lin et al. (2008), here we incorporate the same prescribed lower atmospheric boundary mixing ratio concentrations of greenhouse gases, including methane, for both current and future periods.

In this study, MOZART-2.4 is driven by the meteorological data from the NCAR–DOE PCM (Washington et al. 2000) output at 3-h intervals at T42LR horizontal resolution (~2.8°) and 18 sigma-pressure hybrid levels. Similar or coarser spatial resolutions have been used in recent global modeling studies to project future changes of ozone and/or other pollutants over the United States (e.g., Mickley et al. 2004; MH06; Racherla and Adams 2006; Lin et al. 2008). However, because of the coarse resolution of a global model, these analyses focus on ozone change at the regional scale (i.e., on the order of several hundred kilometers), precluding the resolution of urban or smaller spatial scales.

Present-day precursor emissions for NO_x, carbon monoxide (CO), and nonmethane VOCs are based on the inventories described by Horowitz et al. (2003). The only exceptions are the biofuel and biomass burning emissions of CO, which have been scaled up by a factor of roughly 1.5 to produce a global budget of about 1550 Tg yr^{-1} from all sources, compatible with the estimate of Ehhalt et al. (2001). In particular, the global annual budgets for anthropogenic (including fossil fuel and biofuel) and biomass burning emissions of CO are 677 and 674 TgC, respectively, here; and 650 and 700 TgC, respectively, in Ehhalt et al. (2001). The impact of this scaling on simulated surface ozone concentrations is generally less than 0.5 ppb over both the United States and China.

Biogenic emissions affected by climate change include isoprene emissions from vegetation, which are sensitive to both atmospheric CO_2 concentrations and air temperature, as well as incident solar radiation; terpenes and other VOC emissions (acetone, ethene, ethane, propene, propane, and methanol) from vegetation, which also depend on temperature; and finally, soil emissions of CO which can be modeled as a function of net primary productivity, which is in turn dependent on temperature. The scaling factor of isoprene emissions due to temperature change γ_T was calculated using the equation (after Guenther 1997)

$$\gamma_T = \frac{\exp\left[\dfrac{C_{T1}(T - T_S)}{RT_ST}\right]}{0.961 + \exp\left[\dfrac{C_{T2}(T - T_M)}{RT_ST}\right]}.$$

The scaling factor of isoprene emissions in response to atmospheric CO_2 concentrations [significant at atmospheric concentrations greater than 600 ppm, reached by the A1fi scenario during 2095–99] δ_{ISO} was calculated using the relationship (after Potosnak 2002)

$$\delta_{ISO} = -0.00041[CO_2] + 1.28, \quad \text{if} \quad [CO_2] > 600 \text{ ppm}$$

$$\delta_{ISO} = 1.0, \quad \text{if} \quad [CO_2] \le 600 \text{ ppm}.$$

In addition to air temperature and CO_2 concentrations, isoprene also responds to changes in solar radiation on the surface, which could be altered in the future by climate-driven changes in stratospheric ozone layer, cloud liquid water content, or density, as well as cloud cover and height. However, large uncertainties exist in modeling the effects of regional-scale changes in these quantities on surface solar radiation. In addition, changes in solar radiation have been found to much smaller impacts on isoprene emissions than do changes in air temperature (e.g., Tao et al. 2008). Therefore, for the purpose of estimating future changes in isoprene emissions from vegetation here, we hold incident surface solar radiation fixed at present-day levels.

The scaling factor of terpenes emissions due to temperature change γ_T was calculated using the equation (after Guenther 1997)

$$\gamma_T = \exp[\beta(T - T_S)].$$

The scaling factor of terpenes emissions was also used for biogenic emissions of other VOCs.

Finally, since CO emissions from soil have been found to depend strongly on the net primary production (NPP), the following relationship [based on the relationship between global NPP and temperature first derived by Leith (1975)],

$$\delta_{NPP} = f(T_{FUTURE})/f(T_{CURRENT}), \quad \text{where}$$

$$f(T) = -0.056T^3 + 1.607T^2 + 70.114T + 728.91,$$

TABLE 1. Description of MOZART-2.4 simulations. Anthropogenic emissions of ozone precursors are kept at the present-day levels in all simulations. See the fractional changes in biogenic emissions in Table 4.

Simulation	Year and climate	Biogenic emissions
	With original model setup	
(1) Control	1996–2000	Present day
(2) Climate only (A1fi)	2095–99 A1fi	Present day
(3) Climate only (B1)	2095–99 B1	Present day
(4) Climate + biogenic (A1fi)	2095–99 A1fi	Scaled by A1fi temperature and [CO2]
(5) Climate + biogenic (B1)	2095–99 B1	Scaled by B1 temperature and [CO2]
	With three model improvements	
(6) Present day	1999	Present day
(7) Climate only (A1fi)	2099 A1fi	Present day
(8) Climate only (B1)	2099 B1	Present day
(9) Climate + biogenic (A1fi)	2099 A1fi	Scaled by A1fi temperature and [CO_2]
(10) Climate + biogenic (B1)	2099 B1	Scaled by B1 temperature and [CO_2]

was used as the scaling factor for the NPP changes δ_{NPP} from 1996–2000 to 2095–99, based on temperature only. NPP is also a modeled as a function of precipitation and many other climate-related variables (Adams et al. 2004), but for the purposes of this analysis only the direct temperature-related effects are included. As noted by Adams et al. (2004), the empirical model of Leith (1975) gives reasonable estimates of current global NPP rates, based on plant types implicit in the empirically derived relationship. Future predictions of NPP changes, however, must be qualified, as they do not account for changes in vegetation density and implicitly assume immediate changes in regional vegetation types following a temperature change. Projected changes in NPP were then used to scale soil emissions of CO, which presently contribute to 20% of the total emissions in the United States over the summer months and 17% in China.

We do not include estimates of changes in soil emissions of NO because of the poor understanding of both current emissions as well as likely future changes. NO emissions from soil depend on various factors including surface (soil) temperature, water filled pore space (WFPS), deep soil temperature, fertilization rate, sand percentage, pH, wind speed, and so on (e.g., Schindlbacher et al. 2004; Delon et al. 2007). Schindlbacher et al. (2004) initially found that the temperature dependence of NO emissions from soil was greatly affected by WFPS. Delon et al. (2007) expanded on this to conclude that surface soil temperature and WFPS only explained 45% of the variance of the NO emissions from soil. Inclusion of surface soil temperature, WFPS, deep soil temperature, fertilization rate, sand percentage, pH and wind speed together explained 71% of the variance. Currently, no soil properties other than temperature are available for deriving future changes of NO emissions from soil. Given the lack of information to use in projecting future changes, we assume that NO soil emissions remain fixed at present-day levels.

In this study, five 5-yr simulations were conducted to examine the potential effects of climate and biogenic emissions changes on surface ozone under the A1fi and B1 scenarios, as described in Table 1.

3. Model evaluation

To assess MOZART-2.4 capability to simulate present-day surface ozone concentrations during the summer months, we compare the modeled summer average D8hM of surface ozone concentrations over the contiguous United States during 1996–2000 with the Environmental Protection Agency (EPA) Air Quality System (AQS) rural site measurements. Measurements at urban sites were not used for the comparisons as model resolution precludes simulation of urban areas. If multiple rural measurement sites exist within a given model grid cell, the observations are averaged to create a gridcell mean value that can be directly compared with the modeled value for that specific grid cell, following MH06. To enable a direct comparison, the periodic cubic spline interpolation is applied to the 3-h model outputs to generate ozone concentrations at 1-h intervals for calculating the D8hM ozone (same for other simulations for D8hM ozone). Our preliminary analyses suggest that the interpolation method has an insignificant effect on the diurnal cycle of ozone.

Comparing model-simulated versus observed surface summer ozone, we find that the model is capable of reproducing observed concentrations over most of the western United States, with biases generally smaller than 10 ppb. In contrast, it overpredicts the observations by 10–45 ppb over the eastern United States (Fig. 1a). We are not able to systematically evaluate model performance over China because of the lack of ground-

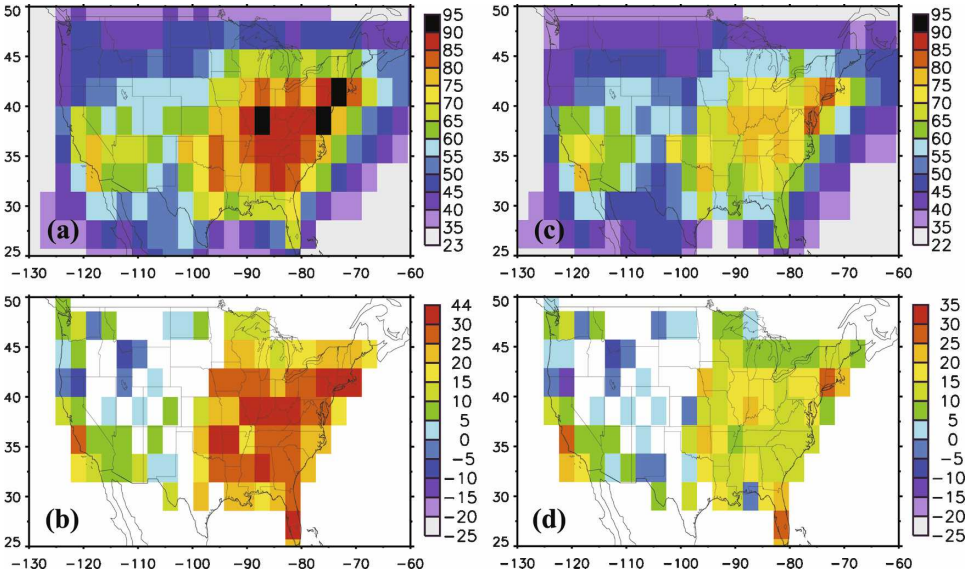

FIG. 1. (a) Summer average daily 8-h maximum surface ozone concentrations (ppb) over the contiguous United States for 1996–2000 in the control MOZART-2.4 simulation with original model setup and (b) the comparisons with the U.S. EPA AQS rural site measurements. (c), (d) The counterparts of (a) and (b), respectively, but for 1999 with model modifications in isoprene nitrate chemistry, dry deposition, and critical Richardson number (see section 3 for details). Positive values in (b) and (d) correspond to overestimations by the model.

level observational data. However, observed summer mean ozone levels at several measurement sites in eastern China, shown in the recent literature, range from 30 to 45 ppb in the late 1990s (e.g., Li et al. 1999; Yan et al. 2003; Wang et al. 2006), about 5–10 ppb lower than the modeled summer mean ozone concentrations averaged over the 3-h model outputs used here.

Similar biases over the eastern United States have been found by MH06 in their MOZART-2.4 simulations for 1990–2000 driven by the Community Climate System Model (CCSM). In addition to the effects of coarse model resolution and errors in emission/meteorological inputs, MOZART-2.4 biases likely result from several specific inaccuracies in model chemistry and physical parameterizations. First, MOZART-2.4 assumes an 8% yield of isoprene nitrates through reactions between nitric oxide and isoprene-derived peroxyl radicals, which then react with hydroxyl radical to completely recycle nitrogen oxides (NO_x = NO + NO_2) rather than converting to nitric acid as a permanent sink of NO_x. More recent studies suggested that the yield of isoprene nitrates as well as the conversion from isoprene nitrates to nitric acid in MOZART-2.4 may be underestimated, leading to the underprediction of the depletion of NO_x through the isoprene nitrate chemistry (see Sprengnether et al. 2002; Fiore et al. 2005 and references therein). In contrast, Horowitz et al. (2007) suggested the best estimate of isoprene nitrate yield to be 4%, of which 40% was recycled back to NO_x, based on the comparison between the simulated and the observed alkyl nitrates within the PBL during an aircraft measurement campaign. However, the results of Horowitz et al. (2007) may have been compromised by the significant positive bias, that is, up to about 70%, in the simulated isoprene concentrations in the PBL.

Second, summertime dry deposition of ozone in MOZART-2.4 is calculated with the resistance-in-series scheme developed by Wesely (1989). Recent observational analyses (Padro 1996; Zhang et al. 1996) and intermodel comparisons (Padro 1996; Zhang et al. 1996; Wesely and Hicks 2000 and references therein) suggest that summertime dry deposition of ozone calculated by the Wesely scheme could be underestimated by at least 30% over deciduous forests in the eastern United States.

Third, boundary layer height could be underpredicted, since the model assigns a critical Richardson number of 0.3. This is smaller than the value of 1.0 that has subsequently been suggested to be more realistic (Stull 1988; Cheng et al. 2002 and references therein).

Therefore, in addition to the five 5-yr simulations, we also conducted five 1-yr simulations to evaluate the impacts of possible model deficiencies on the calculated ozone concentrations and future changes (Table 1). The first run is based in 1999, and the other four are

based in 2099 using the climate and biogenic emissions simulated under the A1fi and B1 scenarios, respectively. In these simulations, three improvements were made in model simulation of isoprene nitrate chemistry, ozone dry deposition, and the critical Richardson number, respectively. Following Fiore et al. (2005), we increase the yield of isoprene nitrate from 8% as used in the original model (i.e., prior to current model improvements) to 12%, at which point it is then converted immediately to nitric acid as the permanent sink of NO_x. A 30% increase of the summertime ozone dry deposition is also applied over the eastern United States only (east of 100°W) as a conservative improvement. The critical Richardson number was adopted as 1.0; in response, the summertime average PBL height was increased by 100–200 m over the United States (not shown). Note that the improvement in ozone dry deposition was only for the eastern United States, while the other two improvements were applied globally.

For the 1999 summertime period, these three improvements reduced model biases to less than 20 ppb over most of the eastern United States (Fig. 1b). The improved isoprene nitrate chemistry had the largest impacts on the ozone simulations over the Southeast, while improvements in the treatment of ozone dry deposition dominates over the Midwest and Northeast, and the improved critical Richardson number dominates along the Northeast coast (not shown). The sensitivity of the projected future ozone changes to model improvements is analyzed in section 5.

4. Results

a. Projected future climate changes

Climate change can affect surface ozone through various ways including changes in air temperature, atmospheric water vapor content, cloud liquid water (CLW) content, lightning frequency, PBL heights, near-surface wind fields, and frontal passages (e.g., Dawson et al. 2007). In this section, we examine these climatic changes from 1996–2000 to 2095–99 as projected by the PCM model under both the A1fi and B1 scenarios.

We first examine the changes in surface air temperature. In general, warmer air temperatures enhance ozone production, leading to faster thermal decomposition of peroxyacetyl nitrate (PAN) and thus increasing concentrations of NO_2 and peroxyacetyl radical (Sillman and Samson 1995; Dawson et al. 2007). Greater warming is projected to occur over the coming century under the higher A1fi scenario as compared to the lower B1 scenario (Fig. 2). By 2095–99 under A1fi, PCM-projected summer mean surface air temperature (calculated as the mean of the 3-h model outputs) increases by more than 6 K over the Rockies, by 3–4 K over most of the eastern United States, and by 2–5 K over eastern China relative to present-day levels. In contrast, PCM-projected temperature increases are less than 2 K over most of the two countries under the lower B1 scenario.

Warmer air temperatures also tend to increase evaporation, which can in turn increase atmospheric water vapor concentrations, leading to more production of hydroxyl radical (OH). More OH can either decrease or increase net ozone production, depending on the relative abundances of NO_x versus odd hydrogen in each region (Sillman and Samson 1995; Racherla and Adams 2006). By 2095–99, projected summer mean near-surface water vapor content increases up to 4 g kg^{-1} over the United States and 3–4 g kg^{-1} over eastern China under the higher A1fi scenario (Fig. 3). In contrast, water vapor increases under B1 are typically less than 1 g kg^{-1} over both countries and are not statistically significant over many areas using the Student's *t* test at the 95% confidence level.

Changes in cloud liquid water content can affect the amount of solar radiation over a region, which can in turn affect the rate of the photochemical reactions involved in the formation of ozone. In addition, the wet deposition of nitrogen species is also influenced by the amount of cloud water. Future changes in cloud water are largely the result of the competition between the increasing air temperature, which tends to decrease the condensation, and the increasing water vapor content, which tends to increase the condensation. By 2095–99 (Fig. 4), PCM-projected summer mean low-level cloud liquid water content (i.e., integrated below 750 hPa in the sigma-pressure hybrid coordinate as these are more relevant to surface ozone than upper-level clouds) increases by up to 5 g m^{-2} over the Northeast and Midwest, and up to 10 g m^{-2} over most of eastern China under A1fi, with decreases as large as 15 g m^{-2} over the northern Great Plains of the United States and 30 g m^{-2} over central China (Fig. 4). In the observational analysis of Del Genio and Wolf (2000), low-level cloud water decreased with increasing air temperature due to reduced cloud thickness over the Great Plains. Under B1, cloud liquid water content is reduced by 0–10 g m^{-2} over most of the United States and central China, with slight increases of up to 10 g m^{-2} over southern China.

Potential changes in the frequency of lightning flashes are primarily a result of projected changes in convection, and can affect the lightning-based production of NO_x in the troposphere. In MOZART-2.4, the lightning production of nitric oxide (LNO) follows the scheme by Price et al. (1997) and Pickering et al. (1998),

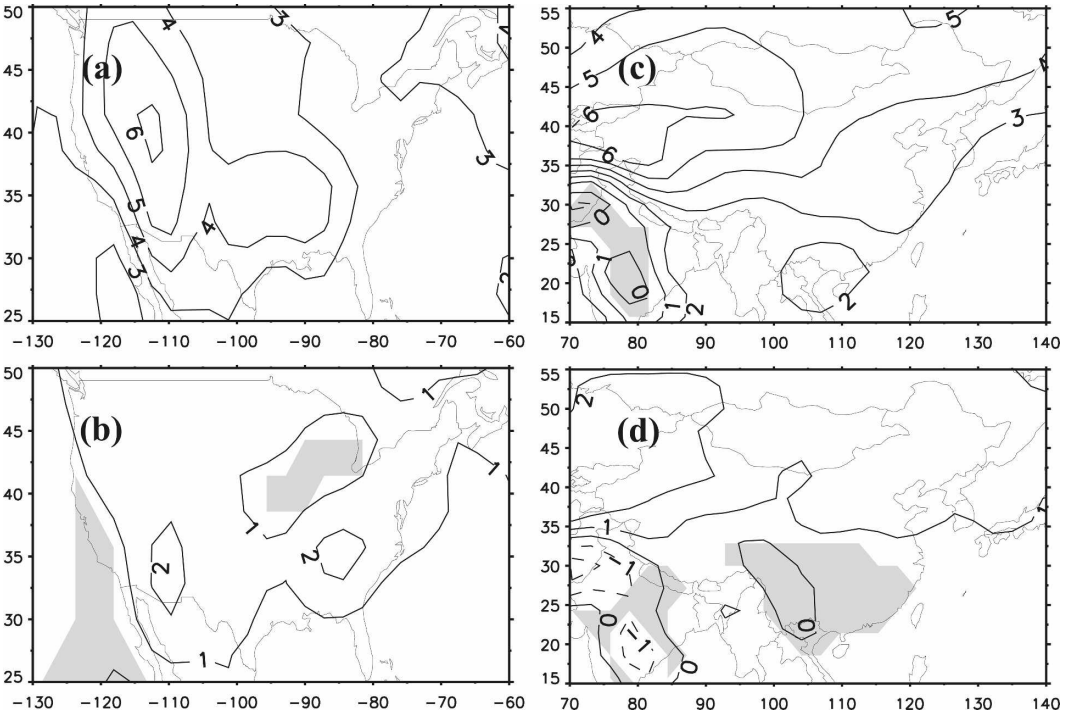

FIG. 2. Changes in June–August average daily mean surface air temperature (K, approximately 0–150 m above the ground) from 1996–2000 to 2095–99 in the United States under (a) A1fi and (b) B1 and in China under (c) A1fi and (d) B1. Solid and dashed contour lines depict higher and lower air temperature in 2095–99 than that in 1996–2000, respectively. The summer average daily means are calculated by averaging the model outputs at 3-h intervals during June–August. Temperature changes in the shaded areas are not significant under the Student's *t* test at the 95% confidence level.

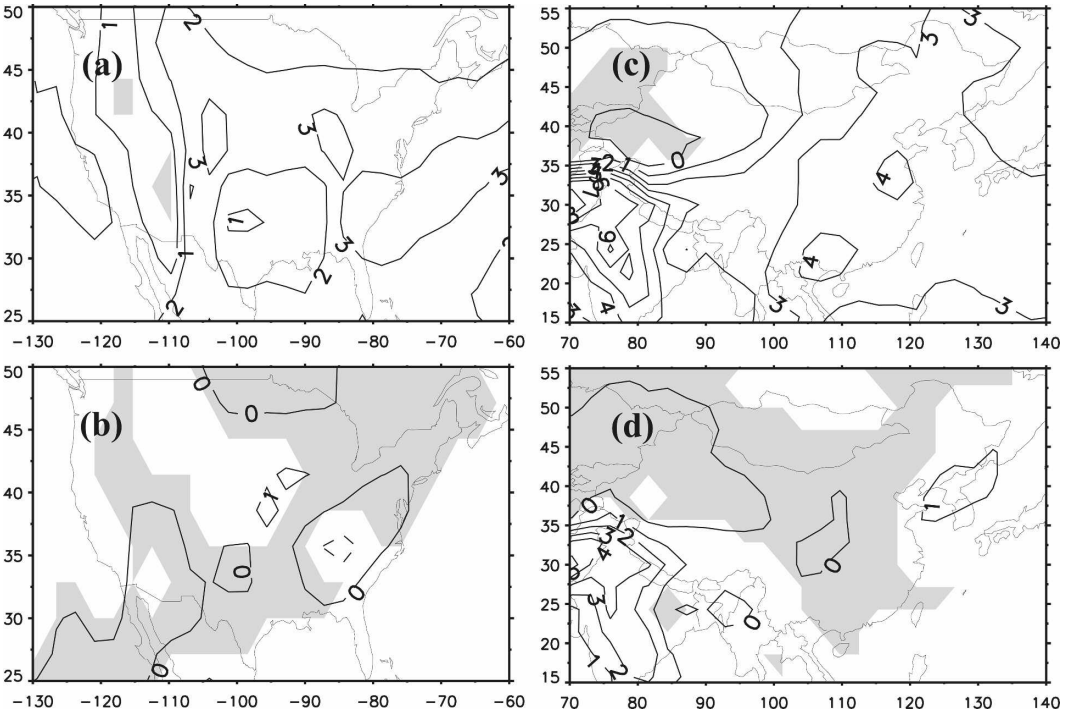

FIG. 3. As in Fig. 2, but for surface water vapor content (g kg^{-1}).

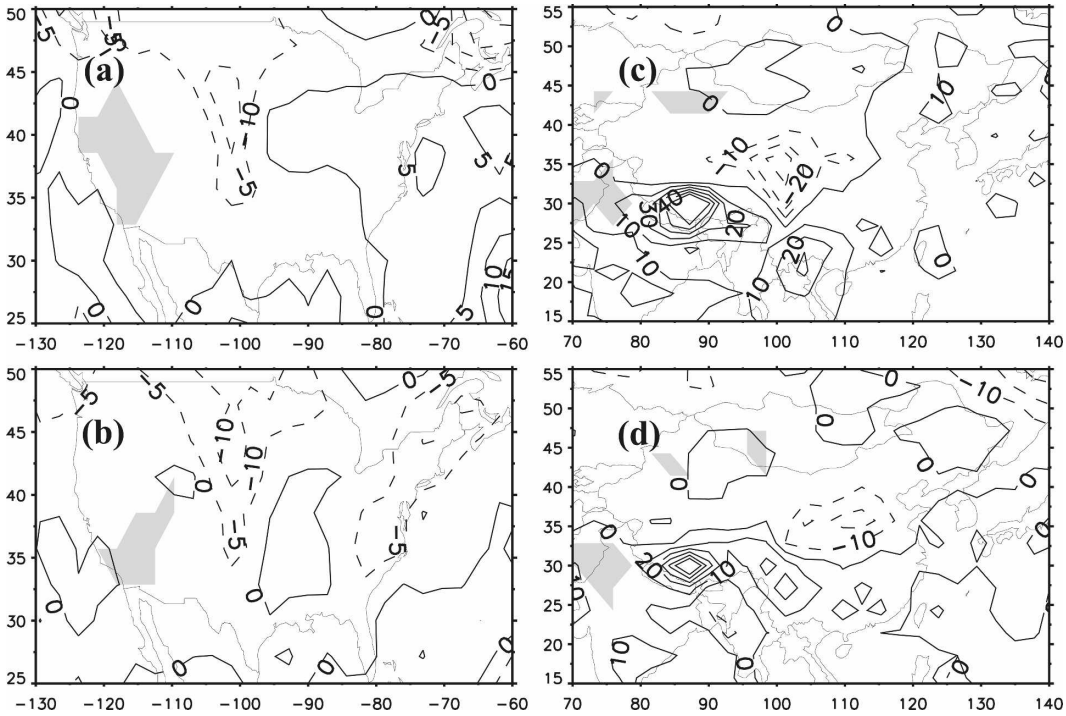

FIG. 4. As in Fig. 2, but for cloud liquid water content (g m^{-2}, integrated below 750 hPa in the sigma–pressure hybrid coordinate). Contour intervals are 5 g m^{-2} in the United States and 10 g m^{-2} in China.

and is highly dependent on cloud height, especially for convective clouds. Globally, summer mean tropospheric LNO increases by 26% under A1fi and 13% under B1 by 2095–99 relative to the budget of 6.7 TgN yr^{-1} during 1996–2000. By comparison, using a coupled climate–chemistry model, Hauglustaine et al. (2005) found that the LNO increased by 50% from 5 TgN yr^{-1} in 2000 to 7.5 TgN yr^{-1} in 2100 under the A2 scenario. Therefore it is consistent among different models and scenarios that, globally, convection is becoming more active and, together with increasing air temperature and water vapor content, is likely to increase LNO over the coming century. Regionally (Fig. 5), summer mean LNO increases by up to 8 GgN yr^{-1} over the Southeast and the central United States and by 4 GgN yr^{-1} over most of eastern China by 2095–99 under A1fi. Under B1, there is an increase as large as 4 GgN yr^{-1} over the central and Midwest United States and a slight decrease over the Southeast. Changes over China under the B1 scenario are generally not statistically significant at the 95% confidence level.

Changes in PBL heights can affect the vertical dilution of ozone. PBL height is dependent on air temperature, water vapor, and winds in the PBL as well as surface sensible and latent heat fluxes. Given the complexity of the PBL mixing processes, there has been no consensus in previous studies on the direction of future changes in PBL heights because of the different parameterizations of PBL mixing and spatial resolutions in various global/regional models as well as the different emission scenarios used to drive the changes (e.g., Hogrefe et al. 2004; Mickley et al. 2004; MH06). For example, Hogrefe et al. (2004) and Mickley et al. (2004) found significant increases in PBL heights over the eastern United States, while MH06 found little. In this study we found that, under A1fi, summer mean PBL heights are projected to decrease up to 100 m over the eastern United States and increase up to 200 m over the Southwest by 2095–99 (Fig. 6), with a decrease of 0–100 m over eastern China. Under B1, by comparison, PBL heights are projected to increase up to 200 m over the eastern United States, with an increase of 0–100 m over most of northern China and a decrease of 0–100 m over southern China.

Changes in wind speed and direction in the lower troposphere affect the horizontal dilution of ozone. Over many coastal areas, especially those with prevailing landward winds, surface ozone concentrations are effectively diluted by marine air masses, since ozone concentrations are usually lower over the nearby oceans. This effect is referred to here as the "marine air dilution effect." Given that both the United States and China have long coastlines, projected changes in landward near-surface winds can have important implica-

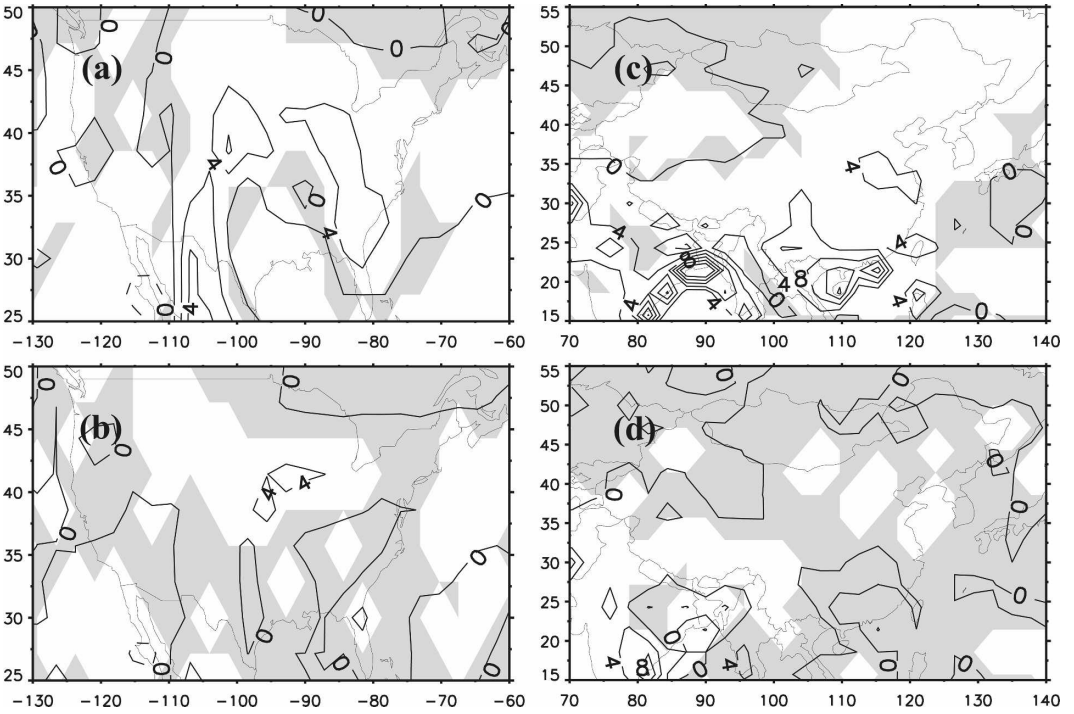

FIG. 5. As in Fig. 2, but for surface LNO (GgN yr^{-1}).

tions for coastal as well as downwind ozone levels. The A1fi and B1 scenarios project distinct changes in near-surface winds from 1996–2000 to 2095–99 (Figs. 7d,e, and 8d,e). Under A1fi (Figs. 7d and 8d), the summer mean low-level jet from the Gulf of Mexico is strengthened and the Asian summer monsoon is intensified (i.e., with stronger southwesterly flows) by 2095–99. This is because of the increased land–ocean thermal

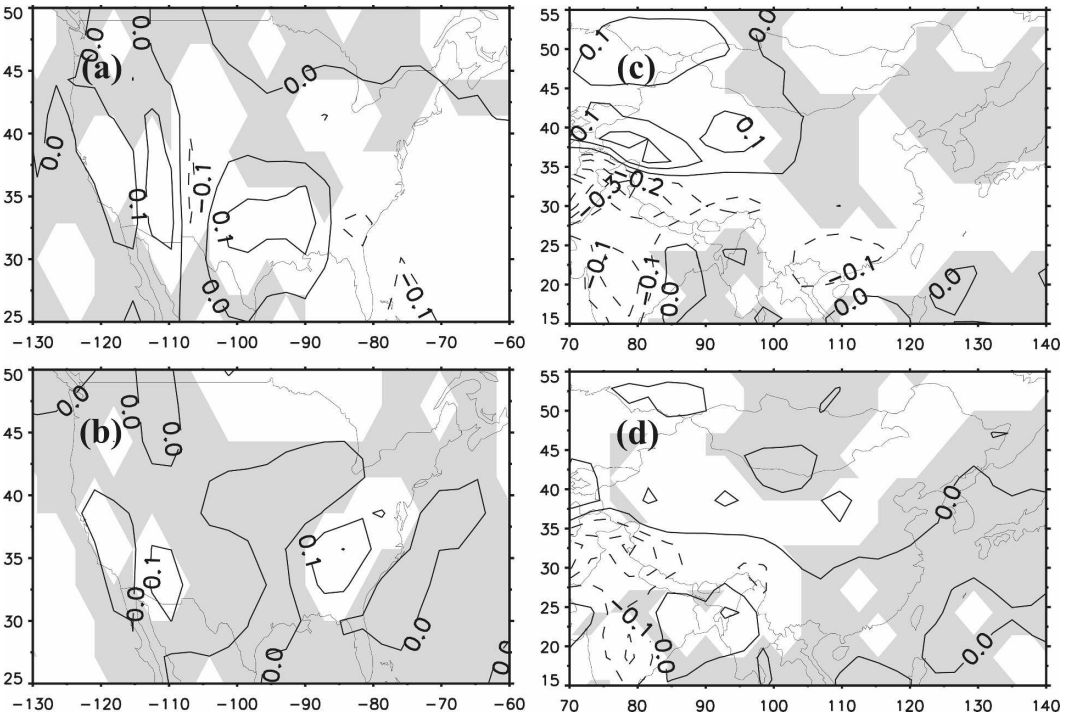

FIG. 6. As in Fig. 2, but for the PBL height (km).

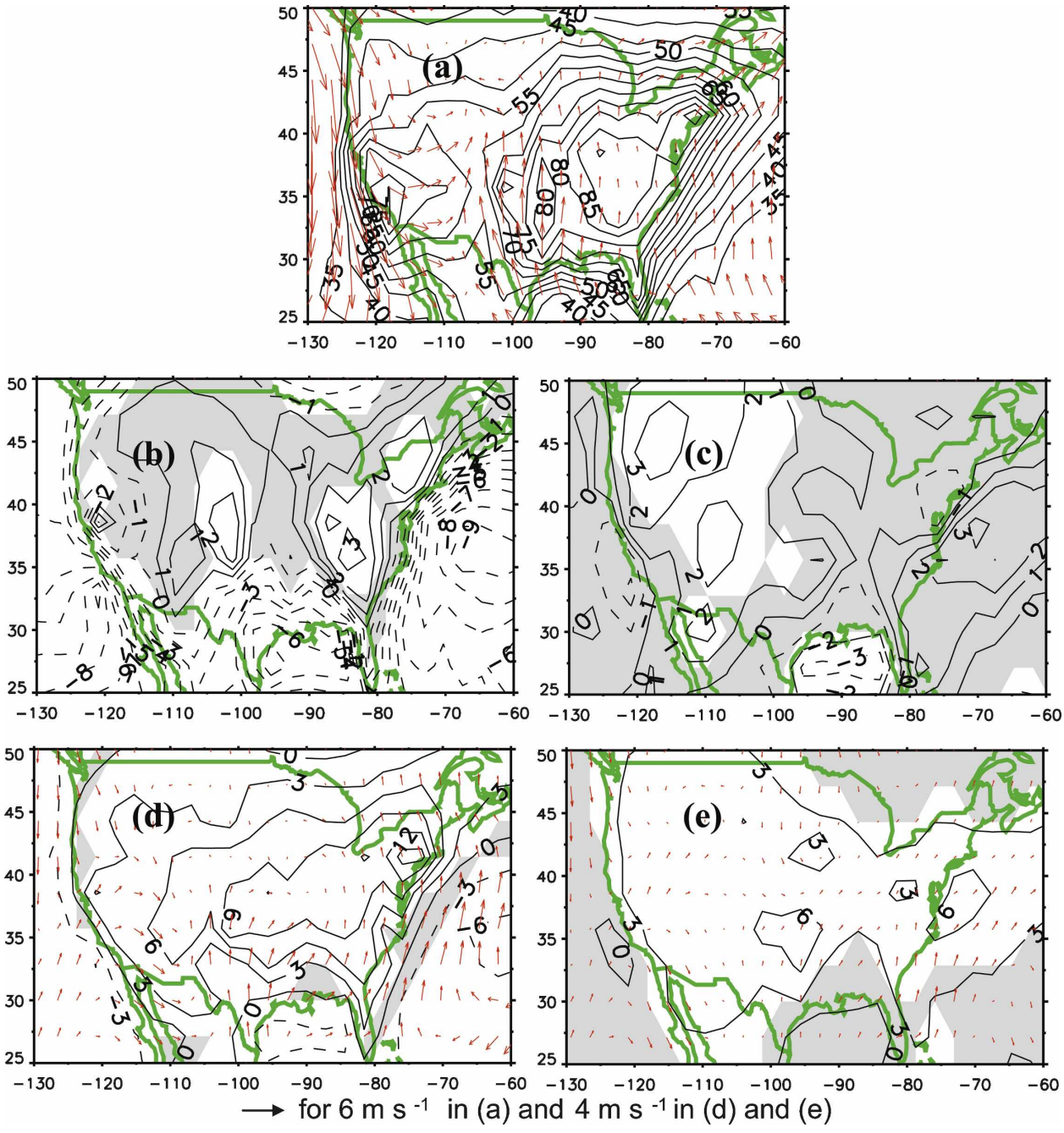

FIG. 7. (a) Summer average daily 8-h maximum surface ozone concentrations (contours, ppb) and daily mean near-surface winds (red arrows) in the United States for the period 1996–2000. Projected ozone changes are for 2095–99 relative to 1996–2000 in response to future projections under (b) A1fi and (c) B1 with climate change only and no changes in biogenic emissions and under (d) A1fi and (e) B1 with changes in climate and biogenic emissions together. Projected changes in near-surface winds are also shown in (d) for A1fi and (e) for B1. The contour intervals are 1 ppb in (b), (c) and 3 ppb in (d), (e). In (b)–(e), solid and dashed contour lines depict higher and lower ozone concentrations in 2095–99 than those in 1996–2000, respectively. Ozone differences in the shaded areas are not significant under the Student's *t* test at the 95% confidence level.

contrast in a warming climate, that is, larger warming over the continents than over the oceans. A strengthened low-level jet from the Gulf of Mexico is also found by MH06 under the A1b scenario, and the intensified Asian summer monsoon is also found by Bueh (2003) for the A2 and B2 scenario and by Bueh et al. (2003) for the IPCC IS92a scenario. As a result, projected landward near-surface winds are stronger along the coasts

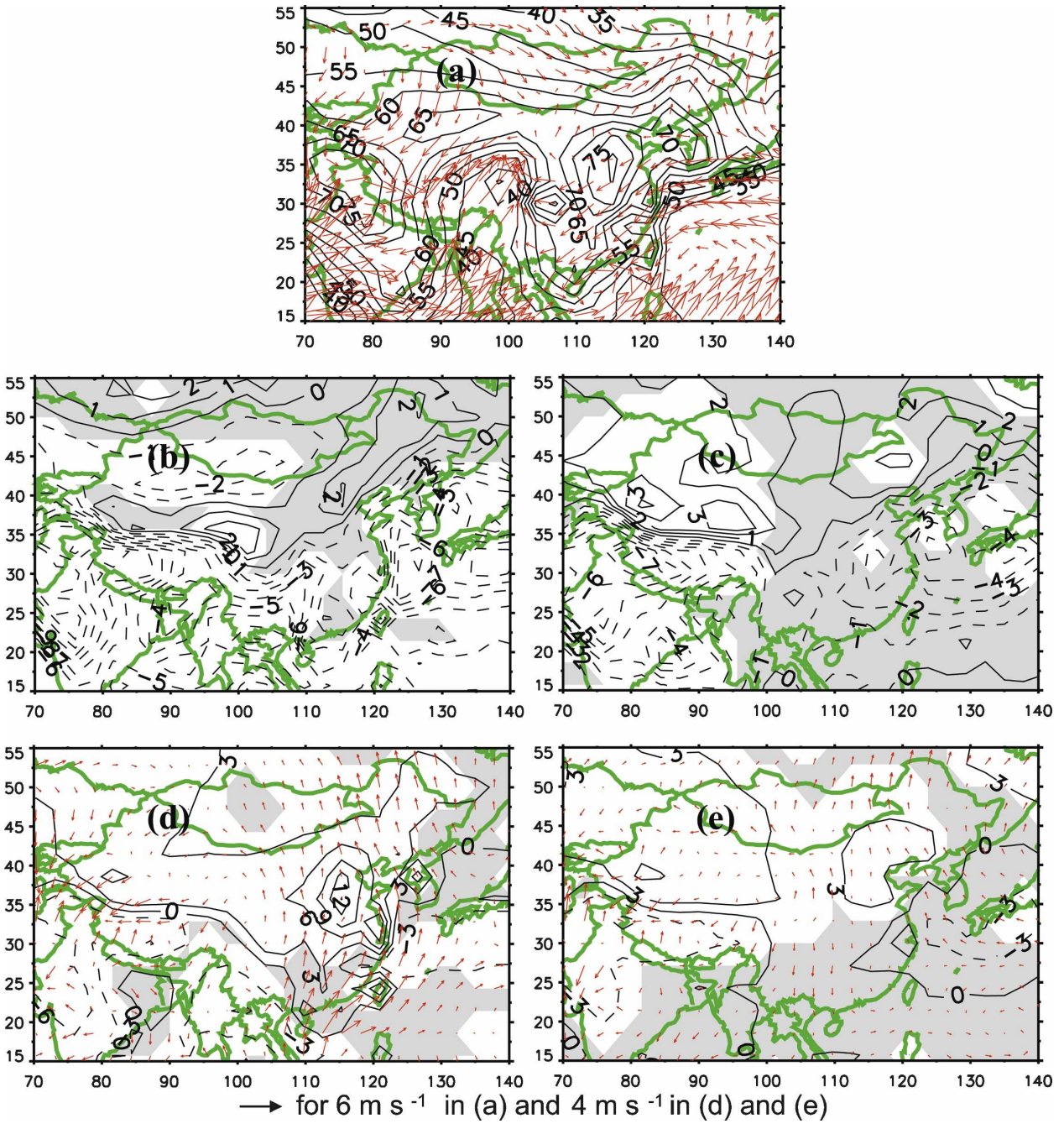

FIG. 8. As in Fig. 7, but for China.

of both countries in future simulations, causing more marine air to be drawn into the continents, enhancing the dilution of coastal ozone concentrations. Under B1 (Figs. 7e and 8e), by comparison, changes in wind fields are less significant than A1fi because of relatively smaller degree of climate change.

In many polluted regions such as the Northeast and Midwest, surface ozone concentrations are effectively mitigated by frontal passages, whose changes in future years will thus have implications for regional pollution levels (Mickley et al. 2004; MH06). Previous studies suggest a potential decrease in the frequency of frontal passages in future years over the Midwest under the A1b scenario (Mickley et al. 2004; MH06). Here we investigate the projected changes in summertime frontal passages under the A1fi and B1 scenarios by com-

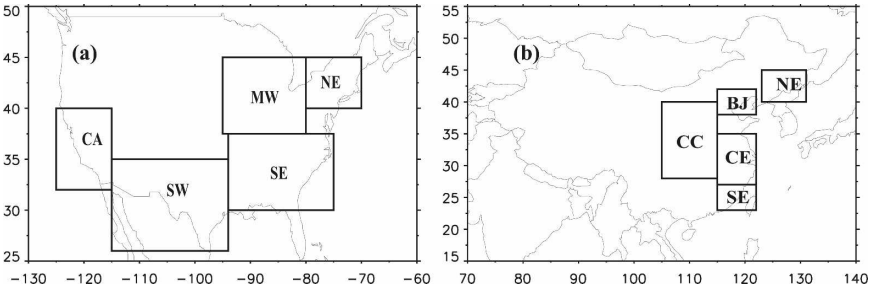

FIG. 9. Boundary specifications of (a) five U.S. regions (Northeast, NE; Midwest, MW; Southeast, SE; California, CA; Southwest, SW) and (b) five Chinese regions (northeast, NE; Beijing area, BJ; central east, CE; southeast, SE; central China, CC). Each region occupies 11–25 model grid cells in the United States and 6–30 grid cells in China; individual grid cells covering neither U.S. nor China lands are not included in the analyses for Figs. 10 and 11.

paring the summertime standard deviations of surface air pressure between 1996–2000 and 2095–99 for each scenario. By 2095–99, changes in the standard deviations are not significant under the Student's t test at the 95% confidence level over the eastern United States and China under either scenario (not shown). Following MH06, we also examine the day-to-day cumulative frequency distributions of surface pressure over the Midwest and Northeast (see boundary specifications in Fig. 9) and find insignificant future changes in regional mean, median, maximum, and minimum in general (not shown). Projected future changes in frontal passages therefore remain uncertain, and may in fact be highly model dependent.

In conclusion, we see significant differences between the A1fi and B1 scenarios for projected future air temperatures, water vapor content, cloud water content, lightning production of NO, PBL height, and near-surface winds, but not for frontal passages. It is clear, therefore, that a number of projected climate-driven changes in key atmospheric characteristics known to affect near-surface ozone concentrations are largely dependent on the climate scenarios used to drive future simulations. For that reason, it is not surprising that our findings as well as those of Hogrefe et al. (2004) (for the A2 scenario) and MH06 (for the A1b scenario) differ from one another.

b. *Projected summer average D8hM ozone changes in response to climate change only*

Simulated June–August average D8hM surface ozone concentrations generally vary from 40–90 ppb over the United States and 50–80 ppb over eastern China during the period 1996–2000 (Figs. 7a and 8a). Along the coasts with landward near-surface winds, ozone is generally diluted by marine air masses. Over eastern China, the winds are so strong that the maximum ozone concentrations are located west (downwind) of emission sources along the coasts. Here, we examine surface ozone responses over the United States and China to future climate changes by 2095–99 under the A1fi and B1 scenarios without including any changes in biogenic emissions (simulations 2 and 3 as described in Table 1, which are compared with simulation 1, the control simulation for the present).

We find that daily mean surface hydroxyl radical (OH) concentrations increase by 0.005–0.03 ppt under A1fi and 0–0.01 ppt under B1 over most of the United States (not shown). Over eastern China, OH concentrations increase by about 0–0.02 ppt under A1fi; under B1, they increase by about 0–0.02 ppt over the northern region (north of 33°N) but show a statistically insignificant decrease of about 0–0.01 ppt over the southern region (not shown).

Under A1fi, the D8hM ozone concentrations increase 1–3 ppb over much of the inland eastern United States and 1–2 ppb over part of northern China from 1996–2000 to 2095–99 (Figs. 7b and 8b). Day-to-day correlations between changes in regional mean surface air temperature and ozone reveal that modeled increases are largely due to warmer air temperatures in future years. Table 2 shows the day-to-day correlations between future changes (2095–99 summers minus 1996–2000 summers) in regional mean surface D8hM ozone and changes in regional mean daily mean air temperature over the Midwest. The correlations were calculated using the following methodology. First, the 460 counts of regional mean D8hM ozone concentrations in current summers (92 counts for each of the five summers) are paired with those in future summers (i.e., 1 June 2095 minus 1 June 1996, 2 June 2095 minus 2 June 1996, and so on, after removing the 5-summer averages for the D8hM ozone during the two periods). A similar procedure is done for regional mean daily mean air

TABLE 2. Cross correlations among June–August day-to-day changes in D8hM ozone and daily mean climate variables from 1996–2000 to 2095–99 over the Midwest. Future changes in ozone are for the experiments with climate change only, i.e., biogenic emissions are not altered. For the climate variables, Ps denotes surface air pressure, *T* denotes air temperature in the lowest model layer (approximately 0–150 m above the ground), *Q* denotes water vapor content in the lowest model layer, PBLH denotes planetary boundary layer height, and CWAT denotes low-level cloud water (integrated below 750 hPa). See section 4b for detailed procedure for calculating such correlations. The numbers before and after the / sign denote the correlations under the A1fi and B1 scenarios, respectively.

	Ozone	Ps	*T*	*Q*	PBLH	CWAT
Ozone	1/1	−0.34/−0.24	0.59/0.63	0.51/0.41	−0.42/−0.31	−0.03/−0.04
Ps		1/1	−0.53/−0.43	−0.51/−0.55	0.30/0.37	−0.05/−0.30
T			1/1	0.57/0.47	−0.13/−0.03	−0.30/−0.23
Q				1/1	−0.75/−0.78	0.19/0.39
PBLH					1/1	−0.37/−0.51
CWAT						1/1

temperature. Then the correlation is calculated between the paired D8hM ozone and the paired daily mean air temperature. Over the Midwest, the value of the correlation can be as large as 0.59, which is greater than the correlations between ozone and other climate variables (see Fig. 9 for regional boundary specifications). Over the Northeast, air temperature also shows the largest correlation with ozone, of all the variables shown in Table 2, 0.74. These findings agree with those of Dawson et al. (2007), who also found that changes in air temperature were the most effective factor for summertime ozone changes over the eastern United States.

By comparison, ozone concentrations decrease by 1–7 ppb along the coastal areas of the two countries by 2095–99 under A1fi (Figs. 7b and 8b). The decreases are largely due to the increased dilution effects of marine air as a result of the enhanced landward winds as well as the reduced oceanic ozone concentrations, which are due to the increased water vapor content at low NO_x levels over the oceans (Sillman and Samson 1995; Johnson et al. 1999). Table 3 presents projected changes in marine air dilution effects on local ozone concentrations averaged over the model grid cells along the oceanic boundaries of the United States and China. To do so, we first identify the "oceanic boundary" grid cells in the two countries. A model grid cell is identified as an oceanic boundary grid cell of the contiguous United States when 1) it covers land that are part of the contiguous United States, and 2) any or all of its four neighbor grid cells (to the south, west, east, north) are oceanic grid cells (i.e., grid cells that are completely over the oceans). The same procedure is done for China. In total, there are 18 oceanic boundary grid cells in the United States and 8 in China at T42 resolution. For each of the oceanic boundary grid cells, we then calculate the advection of ozone in the lowest model layer (approximately 0–150 m above the ground) from neighboring oceanic grid cells when and only when the wind is blowing from neighbor oceanic grid cells to the specified oceanic boundary grid cell. The average of such advection over all oceanic boundary grid cells is then calculated for each country in each period (current and future) as the marine air dilution effects presented in Table 3.

It is a relatively intuitive finding that the negative effects of marine air dilution on coastal ozone concentrations will become stronger by 2095–99 if the ocean–land contrast of ozone concentrations increases and/or the landward winds strengthen. It is shown in Table 3 that on average the enhanced dilution by 2095–99 reduces ozone concentrations by as much as an additional

TABLE 3. June–August mean dilution of coastal ozone concentrations, averaged over the grid cells along the oceanic boundaries, by marine air mass brought by the inland-ward winds (see section 4b for detailed procedure). The unit is parts per billion per day per oceanic boundary grid cell. There are 18 oceanic boundary grid cells along the oceanic boundaries in the United States and 8 in China. Positive values depict that the coastal ozone concentrations are reduced by the marine air dilution. Numbers in the parentheses are the corresponding 5-yr standard deviations. The values for 1996–2000 denote the amounts of the present-day marine air dilution effects and the values for 2095–99 denote changes in marine air dilution effects from 1996–2000 to 2095–99. The numbers shown here are for the lowest model layer (approximately 0–150 m above the ground), while the magnitudes of the dilution are similar within approximately the lowest 500 m above the ground.

	With climate change only	With changes in climate and biogenic emissions
	United States	
1996–2000	5.5 (0.2)	
A1fi 2095–99	2.7 (0.4)	3.3 (0.4)
B1 2095–99	0.8 (0.5)	1.1 (0.5)
	China	
1996–2000	2.9 (0.4)	
A1fi 2095–99	1.3 (0.4)	3.1 (0.5)
B1 2095–99	0.7 (0.5)	1.3 (0.5)

2.7 ppb per day (with a standard deviation of 0.4) beyond present-day levels per oceanic boundary grid cell in the United States and 1.3 ppb per day (also with a standard deviation of 0.4) per oceanic boundary grid cell in China under A1fi. We also calculate advection of ozone for the second lowest model layer (approximately 150–500 m above the ground) and find similar results (not shown). Hence, marine air influences and future changes appear to be consistent in the lower troposphere.

Under B1, different spatial patterns and, in general, smaller changes are seen as compared with A1fi. Surface ozone concentrations increase 1–4 ppb over the western United States and 0–3 ppb over northeastern China from 1996–2000 to 2095–99 (Figs. 7c and 8c). Meanwhile, ozone concentrations decrease 1–3 ppb over the coastal areas surrounding the Gulf of Mexico and 1–4 ppb over most of southeastern China. The ozone changes in eastern China are generally statistically insignificant.

Similar to A1fi, projected future significant ozone increases and decreases under B1 are highly correlated with increased air temperature and increased marine air dilution, respectively. Table 3 shows that, on average, enhanced dilution by 2095–99 reduces ozone levels for the model grid cells along the oceanic boundaries by as much as 0.8 ppb per day per oceanic boundary grid cell in the United States and 0.7 ppb per day per oceanic boundary grid cell in China with a standard deviation of 0.5 ppb for each. As compared to A1fi, the changes in marine air dilution effects under B1 are much smaller over both countries because of the smaller ocean–land contrast of ozone concentrations as well as the smaller changes in near-surface winds.

Projected changes in other climate variables, such as water vapor, cloud liquid water content, lightning, PBL heights, and frontal passages contribute to the ozone changes over the two countries as well. For example, over the Midwest, increases in water vapor content concurrent with increasing air temperatures also enhance ozone concentrations in regions with significant NO_x levels, decreasing PBL height have a positive effect on ozone, while increasing cloud water (under A1fi only) has a negative effect on ozone (Table 2). Quantifying individual contributions of each climate variable to the net ozone change is difficult because of the nonlinear relationships between ozone and these variables (Table 2). Nevertheless, correlations between day-to-day values suggest that increases in surface air temperature and increases in marine air dilution are highly related to the ozone increases over the inland areas and decreases over the coastal areas, respectively, if ozone precursor emissions are held constant.

The spatial pattern of ozone increases over the United States under A1fi found here is similar to the findings by MH06. In their study, summertime average D8hM ozone concentrations increased up to 5 ppb over the inland eastern United States and decreased up to 5 ppb over Texas in response to the projected climate change from 1990–2000 to 2090–2100 under the mid-range A1b scenario. However, there are also some important differences between the two studies. For example, the magnitude of the ozone increase in the Midwest found here is smaller than that found by MH06. This is primarily due to the differences in the climate scenarios and climate models, that is, A1fi and low-sensitivity PCM here versus A1b and higher-sensitivity CCSM in their study. In particular, cloud water was reduced by up to 15 g m^{-2} over the inland eastern United States in their study, but increases by 0–5 g m^{-2} here. Also, cyclone activities over the eastern United States are reduced in future years in their study but are not found to change significantly here. Differences in projected changes of cloud water and cyclone activities likely contribute to the larger ozone change found in their study than here.

c. Projected summer average D8hM ozone changes incorporating changes in climate and biogenic emissions

Projected changes in air temperature and atmospheric CO_2 levels are also expected to affect future biogenic emissions (Guenther 1997), with additional consequences for surface ozone concentrations. Based on the relationships between biogenic emissions, air temperature, and atmospheric CO_2 concentrations described previously in section 2, we project significant global increases from 1996–2000 to 2095–99 in biogenic emissions of isoprene, terpenes, other VOCs, and CO emissions from soil. Projected increases over the continental United States and China are summarized in Table 4. Note that, since the reactivity of CO with OH is much smaller than those of VOCs such as isoprene, CO is not as important as VOCs for surface ozone production over the United States and China; therefore, its future changes have much smaller impacts on ozone than do changes in VOCs.

Incorporating changes in climate and biogenic emissions simultaneously, we find daily mean surface OH concentrations to be reduced by about 0–0.06 ppt under A1fi and 0–0.04 ppt under B1 over most of the two countries (not shown). The magnitudes of surface D8hM ozone changes from 1996–2000 to 2095–99 differ substantially between the two scenarios. Under A1fi,

TABLE 4. Projected fractional changes from 1996–2000 to 2095–99 in biogenic emissions under the SRES A1fi (higher) and B1 (lower) scenarios. The present-day numbers are for the 1996–2000 summer budgets. The units are teragrams of carbon per summer for isoprene, terpenes, and other VOCs, and teragrams per summer for CO.

Species	Contiguous United States			China		
		A1fi	B1	Present day	A1fi	B1
Isoprene	15.5	+93%	+32%	13.2	+94%	+40%
Terpenes and other VOC	10.4	+44%	+15%	7.3	+41%	+15%
CO from soils	4.8	<+1%	<+1%	6.5	<+1%	<+1%

ozone concentrations increase by 1–15 ppb over most of the United States and eastern China, with slight ozone decreases along the coast of the Gulf of Mexico (Figs. 7d and 8d). Under B1, by comparison, ozone concentrations increase by no more than 7 ppb over the United States and no more than 5 ppb over eastern China (Figs. 7e and 8e). To compare our results with Kunkel et al. (2008), we calculate the percentage change of D8hM ozone over the northeastern United States (64°–82°W, 37°–44°N) from 1996–2000 to 2095–99. We find that the ozone changes here are about +12% under the A1fi scenario and +4% under B1, which are within the range of changes they found, that is, 10%–30% for A1fi and 1%–13% for B1.

The relative effects of projected changes in biogenic emissions on ozone as compared to climate change are very different between A1fi and B1. Under A1fi, projected changes in ozone are primarily determined by changes in biogenic emissions. Under B1, in contrast, the relative contributions are not as clear. This is primarily because of the differences between the two scenarios in the magnitudes of projected changes in biogenic emissions. Using a regional model, Hogrefe et al. (2004) found that, although projected biogenic emissions increased by 10%–50% over the eastern United States from the 1990s to the 2050s, the resulting effects on ozone did not exceed the effects from changes in climate. In their study, however, the climate change effects on ozone could have been overestimated, because the same lateral boundary conditions of chemical concentrations were used for both current and future periods. Thus, ozone reductions at the eastern (oceanic) and southern (coastal) boundaries, as shown in our study, as well as their effects, most likely negative, on the ozone levels within the model domain were excluded. Determination of the relative contributions of changes in biogenic emissions to regional ozone concentrations as compared with the contributions from changes in climate alone therefore appears to be highly dependent on the scenarios and modeling approaches used, further explaining some differences between this study and previous ones.

d. Projected changes in the occurrences of high ozone concentrations

One important aspect of future ozone change is in the occurrence of "high ozone concentration" days, that is, the change in the number of days with ozone concentrations exceeding a certain predetermined threshold. Here, we investigate changes in the number of "high" ozone days during June–August from 1996–2000 to 2095–99. For a given region, we first define the threshold of high ozone concentrations as the 85th quantile of the day-to-day cumulative frequency distribution (CFD) of the modeled D8hM ozone during 1996–2000 summers. A day with D8hM ozone exceeding the threshold is identified as a high-ozone day. Note that the threshold is dependent on the specific region being studied. Although selecting the 85th quantile of the CFD as the threshold to define high ozone occurrences is arbitrary, setting the threshold at the 80th and 90th quantile yielded similar findings.

We then focus on the projected changes in high-ozone days over five regions for both the United States (Northeast, Midwest, Southeast, California, Southwest) and China (northeast, Beijing area, central east, southeast, and central China), as defined in Fig. 9. These regions are highly populated, and are already facing potential adverse health effects from elevated surface ozone concentrations. The thresholds of high-ozone days vary from 69–89 ppb for individual regions over the United States and 69–81 ppb over China, but the number of high-ozone days during 1996–2000 summers is fixed at 69, or 15% of the 460 days in the five summers, in any of the 10 regions. For future time periods, however, the threshold remains unchanged for each region, while the number of high-ozone days is allowed to vary.

We first compare modeled with observed numbers of high-ozone days for the present-day period for the five U.S. regions (Fig. 10a). There is no similar comparison for China since the observational data are not available. Given the relatively large model biases, to facilitate the comparison we reconstruct the observed CFD for each

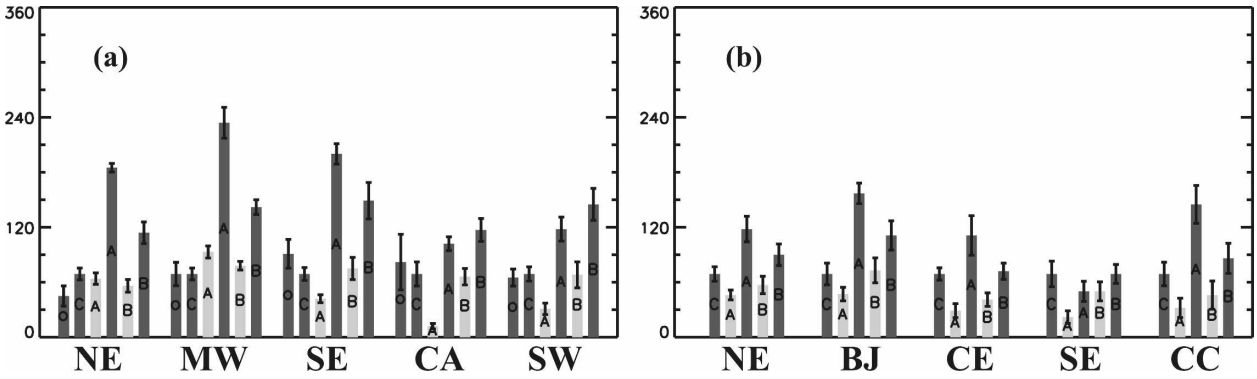

FIG. 10. The number of summertime high-ozone days (±1 std dev; for daily 8-h maximum ozone) during current (1996–2000) and future (2095–99) periods for (a) five U.S. regions and (b) five Chinese regions. See text for the definition of high-ozone days and Fig. 9 for regional boundary specifications. In each region, from left to right, the dark gray bar with symbol "O" in the middle [only available in (a)] depicts the current observed high-ozone days (after reconstructing the observed CFD by adding the difference in the ozone median concentrations between the simulations and observations during 1996–2000); the dark gray bar with symbol "C" depicts the current modeled high-ozone days; the light gray bar with symbol "A" depicts the future high-ozone days under A1fi with climate change only and no changes in biogenic emissions; the dark gray bar with symbol "A" depicts the future high-ozone days under A1fi with changes in climate and biogenic emissions together; the light gray bar with symbol "B" depicts the future high-ozone days under B1 with climate change only and no changes in biogenic emissions; and the dark gray bar with symbol "B" depicts the future high-ozone days under B1 with changes in climate and biogenic emissions together.

region by adding the difference in the ozone median concentrations between the simulations and the observations during 1996–2000, as shown in Fig. 11. The median of the modeled CFD is about 22 ppb larger than the observed median over the Northeast, 25 ppb over the Midwest, 27 ppb over the Southeast, 7 ppb over California, and 13 ppb over the Southwest.

Observed numbers of high-ozone days are significantly lower than the modeled high-ozone days in the Northeast, but higher in the Southeast. This is because modeled ozone concentrations undergo stronger day-to-day variations than the observed in the Northeast but lower variations in the Southeast (Figs. 11a,c). There are no statistically significant differences between the frequency of observed and the modeled high-ozone days over the Midwest, California, and the Southwest.

Considering climate change only and no biogenic emissions perturbations, we see opposing trends of changes in the numbers of high-ozone days from 1996–2000 to 2095–99, depending on location. High-ozone days increase for the Midwest on one side, and decrease for California and southeast China on the other (Fig. 10). In the Midwest, the number of high-ozone days increases to 93 days under A1fi and 78 days under B1, with a standard deviation of 7 and 5, respectively. The increase is largely due to increases in air temperature, as shown in section 4b. By comparison, the number of high-ozone days drops to 12 days (with a standard deviation of 3) in California and 22 (with a standard deviation of 7) in southeast China under A1fi; and to 66 (9) in California and 50 (10) in southeast China under B1. The reductions over these coastal regions are primarily due to the enhanced dilution effects of marine air, as discussed previously in section 4b.

Incorporating changes in climate and biogenic emissions together, the numbers of high-ozone days increase dramatically beyond the present-day level by 2095–99 over most regions except southeast China (Fig. 10). Increases are more significant under the A1fi than B1 scenario except over California, the Southwest, and southeast China. Over the Midwest, the increase is so large under A1fi that about one-half of the summer days are identified as the high-ozone days in future years. In southeast China, however, effects of changes in biogenic emissions on ozone are largely balanced by effects of increases in marine air dilution; therefore, changes in high-ozone days are insignificant in future years.

e. Projected changes in the day-to-day distributions of D8hM ozone concentrations

We next compare projected changes in regional mean day-to-day CFDs of the D8hM ozone between 1996–2000 and 2095–99 summers over the four U.S. regions: Northeast, Midwest, Southeast, and California (Fig. 11). The other six U.S. or Chinese regions are not shown since the main findings for them are similar to those for the four regions presented here.

With climate change only and no changes in biogenic emissions, projected future ozone changes are generally less than 5 ppb over the entire CFDs in all four regions,

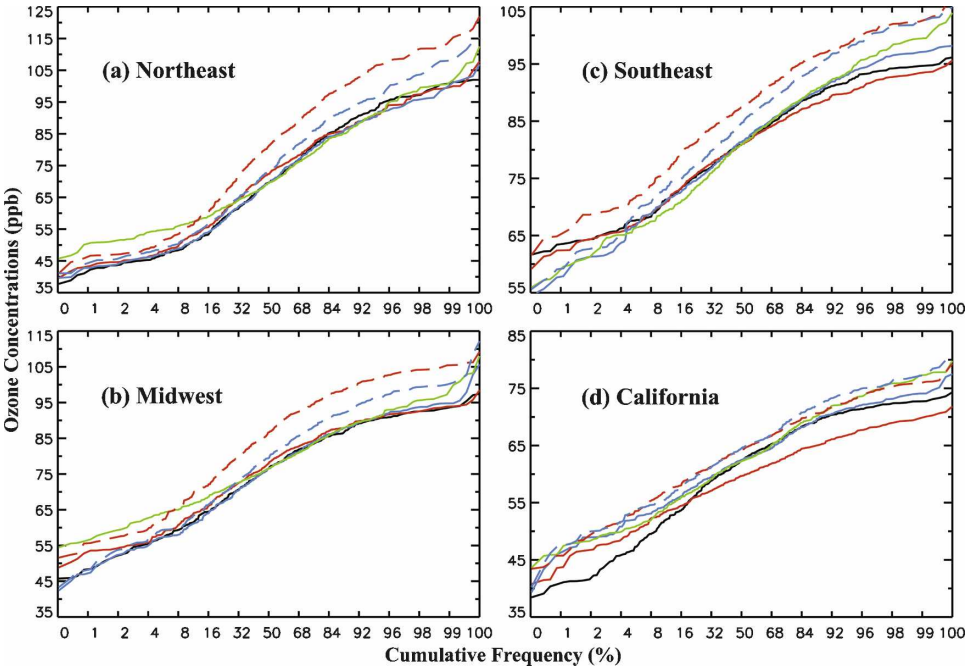

FIG. 11. June–August CFDs of regional mean daily 8-h maximum ozone concentrations during 1996–2000 and 2095–99 over the four U.S. regions: (a) northeast, (b) midwest, (c) southeast, and (d) California. See Fig. 9 for regional boundary specifications. In each region, the green solid line depicts the observed CFD during 1996–2000 (after adding the difference in the ozone median concentrations between the simulations and observations during 1996–2000), the black solid line depicts the modeled CFD during 1996–2000, the red solid line depicts the modeled CFD during 2095–99 under A1fi with climate change only and no changes in biogenic emissions, the red dashed line depicts the modeled CFD during 2095–99 under A1fi with changes in climate and biogenic emissions together, the blue solid line depicts the modeled CFD during 2095–99 under B1 with climate change only and no changes in biogenic emissions, and the blue dashed line depicts the modeled CFD during 2095–99 under B1 with changes in climate and biogenic emissions together. Note that the scales of *y* axes are different for the four regions in order to show the ozone changes more clearly.

and few are statistically significant at the 95% confidence level based on the two-sample quantile test (Fig. 11). Over the Northeast, there is no statistically significant ozone change under either the higher or lower emissions scenario. Over the Midwest, ozone concentrations increase up to 5 ppb at the 1st quantile of the CFD under A1fi. Under B1, there is no statistically significant ozone change except the increase above the 99th percentile. Over the Southeast, there is no statistically significant ozone change under A1fi whereas under B1, only the decrease below the 2nd percentile and the increase above the 98th percentile are statistically significant. Over California, ozone concentrations decrease around 5 ppb at most of the CFD above the 20th percentile and increase up to 5 ppb at the lower tail of the CFD under A1fi. Under B1, there is no statistically significant ozone change at the upper tail of the CFD except above the 99th percentile, while the increase at the lower tail is larger than that under A1fi. Overall we find that the ozone changes from 1996–2000 to 2095–99 are not limited to the upper tail of the CFDs over the four regions. We also examine the changes in ozone CFD for individual model grid cells within each region and find similar results. Similarly, MH06 constructed the CFDs of daily mean ozone for regional maximum, median, and minimum, respectively, over a region in the central and eastern United States (35°–45°N, 96°–80°W) as well as the CFDs for individual model grid cells within the region. They also found that ozone concentrations increased throughout the CFD from the 1990s to the 2090s under the midrange A1b scenario. In contrast, using a global model to study climate change effects on black carbon and CO (no changes in biogenic emissions), Mickley et al. (2004) found that changes in pollutant concentrations from 1995–2002 to 2045–52 under the A1b scenario were significant at and only at the upper tail of the CFDs over the Northeast and Midwest. The differences between our and their findings can be explained by the differences in climate and chemistry models as well as climate scenarios. For ex-

ample, the spatial resolution here (2.9° latitude × 2.8° longitude with 18 vertical layers) is much higher than that in Mickley et al. (2004) (4° latitude × 5° longitude with nine vertical layers).

When changes in both climate and biogenic emissions are incorporated, surface ozone concentrations significantly increase from 1996–2000 to 2095–99, more so under A1fi than B1 primarily because of much larger increases in biogenic emissions. Under both scenarios, ozone concentrations increase throughout the CFDs, although increases tend to be greater toward the upper tail of the CFDs over most regions. By comparison, Hogrefe et al. (2004), who also considered climate change and biogenic emissions perturbations using a regional modeling framework, found little ozone change at the lower tail of the CFDs over the Northeast and Midwest with changes in climate and biogenic emissions as projected under the mid–high A2 scenario. Again, in addition to the distinctive climate–emission scenarios used, the differences between our and their findings are also due to the different climate and chemical modeling approaches, as discussed in section 4c.

5. Sensitivity of ozone changes to model improvements

Last we compare the simulated D8hM ozone changes over the United States and China from 1999 to 2099 with and without the three improvements in model chemistry–physics discussed previously in section 3. With climate change only and no biogenic emissions perturbations, these model improvements have minor effects (mostly less than 1 ppb) on projected future surface ozone changes over the United States (not shown). Incorporating changes in both climate and biogenic emissions, however, the projected ozone changes with model improvements are about 1–7 ppb smaller under A1fi and about 0–4 ppb smaller under B1 (Fig. 12) than the ozone changes without model improvements. Under A1fi, the improved model produces ozone decreases over the northern and southern Great Plains because of the increasing biogenic emissions alone (not shown). Similarly, over eastern China, the projected ozone changes due to climate change alone are affected insignificantly by the model improvements; while the ozone increases as a result of changes in climate and biogenic emissions together are about 2–7 ppb smaller under A1fi and about 1–3 ppb smaller under B1 when the model improvements are incorporated (not shown). This is because when biogenic emissions are greatly increased, the improved isoprene–nitrate chemistry results in more reduction of NO_x and thus less ozone production. Therefore the magnitude of projected ozone change in response to biogenic emissions changes is sensitive to the treatment of isoprene nitrates. Nevertheless, under A1fi, the effects of biogenic emissions changes on ozone are still much larger than the effects of climate change over most of the United States and eastern China.

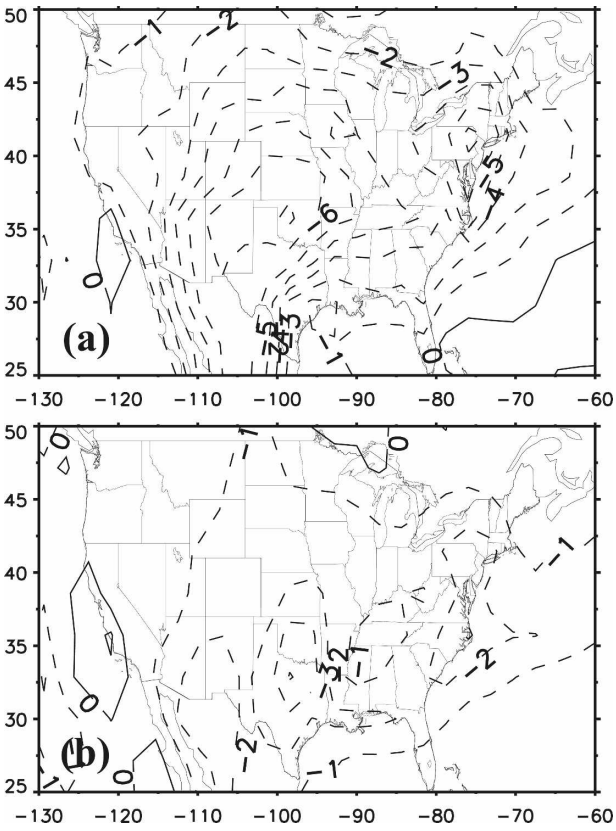

FIG. 12. Differences between the projected changes in summer average daily 8-h maximum ozone concentrations over the United States from 1999 to 2099 due to changes in climate and biogenic emissions together under (a) A1fi and (b) B1, with and without the three model improvements (see section 3 for details). Negative values (dashed lines) denote that the projected ozone changes are smaller when the three model improvements are incorporated.

6. Conclusions and discussion

This study analyzes the results of a series of MOZART-2.4 CTM simulations to project summertime surface ozone changes over the United States and China for the period 2095–99 relative to 1996–2000 in response to changes in climate and biogenic emissions projected by the PCM climate boundary conditions corresponding to the IPCC SRES A1fi (higher) and B1 (lower) emission scenarios. When compared with the EPA AQS rural site measurements during 1996–2000, MOZART-2.4 simulations are able to reproduce ob-

served surface daily 8-h maximum ozone concentrations over most of the western United States with biases generally less than 10 ppb, but overestimate ozone levels by 10–45 ppb over the eastern United States. These biases are at least partially attributable to inaccuracies in model chemistry and physical parameterizations.

Over both the United States and China, projected changes in climate, including air temperature, water vapor content, cloud liquid water content, lightning frequency, boundary layer heights, wind fields, and frontal passages, as well as corresponding changes in biogenic emissions, differ significantly between the A1fi and B1 scenarios. It is therefore not surprising that CTM simulations using climate-related changes as projected under the A1fi and B1 scenarios result in very different projections of regional ozone change. These results highlight the importance of the future scenario used to drive projected climate change when assessing likely changes in future near-surface ozone concentrations.

Considering climate change only and no changes in biogenic emissions, changes in summer average D8hM ozone concentrations by 2095–99 relative to present-day levels are mostly less than 3 ppb over the United States and China under both scenarios. Over the United States, ozone concentrations increase in much of the inland eastern part of the country under A1fi and in the western half of the country under B1. Coastal ozone levels are reduced under both scenarios, although more significantly under A1fi. Over eastern China, ozone concentrations increase in the northern area and decrease in the southern area under both scenarios.

Defining "high-ozone days" as lying above the 85th quantile of the present-day summer day-to-day D8hM ozone distribution, we find that the number of high-ozone days greatly increases over the Midwest from 69 to 93 under A1fi and to 78 under B1. In contrast, the number of high-ozone days decreases over the coastal regions of California, from 69 to 12 under A1fi and to 66 under B1, and southeast China, from 69 to 22 under A1fi and to 50 under B1. While effects of changes in other climate variables cannot be ruled out, we find that ozone increases in inland areas are highly correlated with increases in air temperature, while ozone decreases in coastal areas are highly correlated with increased dilution effects by marine air masses.

When changes in climate and biogenic emissions are incorporated together, the difference between the A1fi and B1 scenarios is more pronounced. Not only do the spatial patterns of change vary between the two scenarios, but the projected magnitude of ozone change differs greatly as well. Over both countries, summertime average surface D8hM ozone concentrations increase 1–15 ppb under A1fi but only 0–7 ppb under B1. Also, the number of high-ozone days increases dramatically. This increase is so large over the Midwest that about one-half of summer days are identified as the high-ozone days by the end of the twenty-first century under A1fi.

Further analysis of the cumulative frequency distributions of daily summertime ozone reveals that the projected ozone changes are not limited to the upper tail of the cumulative frequency distributions of day-to-day ozone variations under either scenario, but occur across most, if not all, of the distribution. Our findings are similar to those of MH06, but disagree with the findings by Mickley et al. (2004) and Hogrefe et al. (2004), who projected ozone changes to mainly occur at the upper tail of the CFDs. This disagreement is likely due to the differences in modeling approaches as well as climate–emission scenarios used.

Corrections to potential inaccuracies in model physics–chemistry—specifically, improvements in isoprene nitrate chemistry, ozone dry deposition, and critical Richardson number—have important implications for ozone projections. With climate change only, the projected future ozone change is affected insignificantly by these corrections. Considering changes in both climate and biogenic emissions, however, the projected D8hM ozone change over the United States decreases by about 1–7 ppb under the A1fi scenario and about 0–4 ppb under B1 when the model improvements are incorporated, as compared to the projected ozone changes without model improvements. This is primarily because the increasing biogenic emissions lead to decreasing NO_x concentrations when the isoprene nitrate chemistry is improved. Nevertheless, changes in biogenic emissions remain the dominant factor of future ozone change as compared to the effects of climate change even under the A1fi scenario.

There are several limitations in this study. Because of the coarse resolution of the current global climate and chemical transport models used here, we were not able to examine detailed projections of future ozone changes at the urban or smaller scales. To accomplish these tasks, an integrated modeling system combining global and regional emission–climate–chemistry models is required. We are currently implementing the system (Huang et al. 2007, manuscript submitted to *J. Geophys. Res.*) with the global CTM simulations presented here used as time-dependent boundary conditions for regional air quality model. Also, the effects of changes in land use types and solar radiation on biogenic emissions were not considered in the present study. In addition, the effects of changes in OH on methane are not fully accounted for in this study because of the pre-

scribed lower atmospheric boundary condition for methane. This, however, is not expected to significantly affect the projected ozone changes, given the much lower reactivity of methane with OH as compared with other VOCs and CO. Furthermore, as noted previously, the sensitivity of the PCM model to greenhouse gas emissions is at the lowest end of the currently accepted range. Hence, the magnitude of the projected changes estimated here, particularly those related to air temperature, may represent a highly conservative estimate of what might actually be expected under a given emissions scenario.

Despite these limitations, however, the results of this study allow us to draw several important conclusions regarding projected future ozone concentrations over the contiguous United States and eastern China. First, we find that future changes in climate are likely to significantly impact summertime near-surface ozone concentrations both over the United States, which currently experiences a peak in annual ozone concentrations during the summer months, as well as over east China, which does not because of the marine air dilution effect associated with the Asian summer monsoon. Furthermore, in coastal areas, much of the ozone change can be attributed to increased transport of marine air masses into the region rather than in situ production. Second, the climate warming is not only expected to increase the frequency of high-ozone days, but is also projected to occur across the distribution of daily 8-h maximum ozone. Third, our simulations indicate that the secondary effects of human-induced climate change on future near-surface ozone concentrations, as illustrated here by projected changes in biogenic emissions, are likely to be even larger than the direct effects of climate change itself (i.e., due to changes in air temperature, humidity, atmospheric circulation, etc). And, last and perhaps most important, our results quantify the large uncertainty in future ozone changes due to the different climate/emission scenarios used. In general, significantly (and not always linearly) greater changes were seen under the SRES higher (A1fi) scenario as compared with the lower (B1) scenario, highlighting the importance of input scenarios in determining the outcome of a given modeling study.

Acknowledgments. The research was supported in part by the U.S. Environmental Protection Agency Science to Achieve Results (STAR) Program under award number EPA RD-83096301-0. The authors acknowledge DOE/NERSC and NCSA/UIUC for the supercomputing support. We thank Larry Horowitz and Daeok Youn for discussions on the model performance and uncertainties; and Xu-Ming He and Xiao-Feng Shao for discussions on the statistical tests. The views expressed are those of the authors and do not necessarily reflect those of the sponsoring agencies and other organizations, including Illinois State Water Survey.

REFERENCES

Adams, B., A. White, and T. Lenton, 2004: An analysis of some diverse approaches to modelling terrestrial net primary productivity. *Ecol. Modell.,* **177,** 353–391.

Bueh, C., 2003: Simulation of the future change of Asian monsoon climate using the IPCC SRES A2 and B2 scenarios. *Chin. Sci. Bull.,* **48,** 1024–1030.

——, U. Cubasch, and S. Hagemann, 2003: Impacts of global warming on changes in the East Asian monsoon and the related river discharge in a global time-slice experiment. *Climate Res.,* **24,** 47–57.

Cheng, Y., V. M. Canuto, and A. M. Howard, 2002: An improved model for the turbulent PBL. *J. Atmos. Sci.,* **59,** 1550–1565.

Dawson, J. P., P. J. Adams, and S. N. Pandis, 2007: Sensitivity of ozone to summertime climate in the eastern USA: A modeling case study. *Atmos. Environ.,* **41,** 1494–1511.

Del Genio, A. D., and A. B. Wolf, 2000: The temperature dependence of liquid water path of low clouds in the southern Great Plains. *J. Climate,* **13,** 3465–3486.

Delon, C., D. Serca, C. Boissard, R. Dupont, A. Dutot, P. Laville, P. D. Rosnay, and R. Delmas, 2007: Soil NO emissions modelling using artificial neural network. *Tellus,* **59B,** 502–513.

Denman, K. L., and Coauthors, 2007: Couplings between changes in the climate system and biogeochemistry. *Climate Change 2007: The Physical Science Basis,* S. Solomon et al., Eds., Cambridge University Press, 499–588.

Ehhalt, D., and Coauthors, 2001: Atmospheric chemistry and greenhouse gases. *Climate Change 2001: The Scientific Basis,* J. T. Houghton et al., Eds., Cambridge University Press, 239–287.

Fiore, A. M., L. W. Horowitz, D. W. Purves, H. Levy II, M. J. Evans, Y. Wang, Q. Li, and R. M. Yantosca, 2005: Evaluating the contribution of changes in isoprene emissions to surface ozone trends over the eastern United States. *J. Geophys. Res.,* **110,** D12303, doi:10.1029/2004JD005485.

Guenther, A., 1997: Seasonal and spatial variations in natural volatile organic compound emissions. *Ecol. Appl.,* **7,** 34–45.

Hauglustaine, D. A., J. Lathière, S. Szopa, and G. A. Folberth, 2005: Future tropospheric ozone simulated with a climate–chemistry–biosphere model. *Geophys. Res. Lett.,* **32,** L24807, doi:10.1029/2005GL024031.

Hogrefe, C., and Coauthors, 2004: Simulating changes in regional air pollution over the eastern United States due to changes in global and regional climate and emissions. *J. Geophys. Res.,* **109,** D22301, doi:10.1029/2004JD004690.

Horowitz, L. W., and Coauthors, 2003: A global simulation of tropospheric ozone and related tracers: Description and evaluation of MOZART, version 2. *J. Geophys. Res.,* **108,** 4784, doi:10.1029/2002JD002853.

——, and Coauthors, 2007: Observational constraints on the chemistry of isoprene nitrates over the eastern United States. *J. Geophys. Res.,* **112,** D120S8, doi:10.1029/2006JD007747.

Johnson, C. E., W. J. Collins, D. S. Stevenson, and R. G. Derwent, 1999: Relative roles of climate and emissions changes on fu-

ture tropospheric oxidant concentrations. *J. Geophys. Res.,* **104** (D15), 18 631–18 645.

Kunkel, K. E., and Coauthors, 2008: Sensitivity of future ozone concentrations in the northeast U.S.A. to regional climate change. *Mitig. Adapt. Strat. Global Change,* **13,** 597–606.

Lamarque, J.-F., P. Hess, L. Emmons, L. Buja, W. Washington, and C. Granier, 2005: Tropospheric ozone evolution between 1890 and 1990. *J. Geophys. Res.,* **110,** D08304, doi:10.1029/2004JD005537.

Leith, H., 1975: Modeling the primary productivity of the world. *Primary Productivity of the Biosphere,* H. Leith and R. H. Whittaker, Eds., Springer-Verlag, 237–263.

Li, X., Z. He, X. Fang, and X. Zhou, 1999: Distribution of surface ozone concentration in the clean areas of China and its possible impact on crop yields. *Adv. Atmos. Sci.,* **16,** 154–158.

Lin, J.-T., D. J. Wuebbles, and X.-Z. Liang, 2008: Effects of intercontinental transport on surface ozone over the United States: Present and future assessment with a global model. *Geophys. Res. Lett.,* **35,** L02805, doi:10.1029/2007GL031415.

Mauzerall, D. L., D. Narita, H. Akimoto, L. Horowitz, S. Walters, D. A. Hauglustaine, and G. Brasseur, 2000: Seasonal characteristics of tropospheric ozone production and mixing ratios over East Asia: A global three-dimensional chemical transport model analysis. *J. Geophys. Res.,* **105** (D14), 17 895–17 910.

Meehl, G. A., and Coauthors, 2007: Global climate projections. *Climate Change 2007: The Physical Science Basis,* S. Solomon et al., Eds., Cambridge University Press, 747–846.

Mickley, L. J., D. J. Jacob, B. D. Field, and D. Rind, 2004: Effects of future climate change on regional air pollution episodes in the United States. *Geophys. Res. Lett.,* **31,** L24103, doi:10.1029/2004GL021216.

Murazaki, K., and P. Hess, 2006: How does climate change contribute to surface ozone change over the United States? *J. Geophys. Res.,* **111,** D05301, doi:10.1029/2005JD005873.

Padro, J., 1996: Summary of ozone dry deposition velocity measurements and model estimates over vineyard, cotton, grass, and deciduous forest in summer. *Atmos. Environ.,* **13,** 2363–2369.

Pickering, K. E., Y. Wang, W.-K. Tao, C. Price, and J.-F. Müller, 1998: Vertical distributions of lighting NO_x for use in regional and global chemical transport models. *J. Geophys. Res.,* **103,** 31 203–31 216.

Pochanart, P., H. Akimoto, Y. Kinjo, and H. Tanimoto, 2002: Surface ozone at four remote island sites and the preliminary assessment of the exceedences of its critical level in Japan. *Atmos. Environ.,* **36,** 4235–4250.

Potosnak, M., 2002: Effects of growth carbon dioxide concentration on isoprene emissions from plants. Ph.D. thesis, Columbia University, 140 pp.

Prentice, I. C., and Coauthors, 2001: The carbon cycle and atmospheric carbon dioxide. *Climate Change 2001: The Scientific Basis,* J. T. Houghton et al., Eds., Cambridge University Press, 183–237.

Price, C., J. Penner, and M. Prather, 1997: NO_x from lightning. 1. Global distribution based on lightning physics. *J. Geophys. Res.,* **102,** 5929–5941.

Racherla, P. N., and P. J. Adams, 2006: Sensitivity of global tropospheric ozone and fine particulate matter concentrations to climate change. *J. Geophys. Res.,* **111,** D24103, doi:10.1029/2005JD006939.

Schindlbacher, A., S. Zechmeister-Boltenstern, and K. Butterbach-Bahl, 2004: Effects of soil moisture and temperature on NO, NO_2, and N_2O emissions from European forest soils. *J. Geophys. Res.,* **109,** D17302, doi:10.1029/2004JD004590.

Sillman, S., and P. J. Samson, 1995: Impact of temperature on oxidant photochemistry in urban, polluted rural and remote environments. *J. Geophys. Res.,* **100,** 11 497–11 508.

Sprengnether, M., K. L. Demerjian, N. M. Donahue, and J. G. Anderson, 2002: Product analysis of the OH oxidation of isoprene and 1, 3-butadiene in the presence of NO. *J. Geophys. Res.,* **107,** 4268, doi:10.1029/2001JD000716.

Steiner, A. L., S. Tonse, R. C. Cohen, A. H. Goldstein, and R. A. Harley, 2006: Influence of future climate and emissions on regional air quality in California. *J. Geophys. Res.,* **111,** D18303, doi:10.1029/2005JD006935.

Stull, R. B., 1988: *An Introduction to Boundary Layer Meteorology.* Kluwer Academic, 666 pp.

Tao, Z., S. M. Larson, D. J. Wuebbles, A. Williams, and M. Caughey, 2003: A summer simulation of biogenic contribution to ground-level ozone over the continental United States. *J. Geophys. Res.,* **108,** 4404, doi:10.1029/2002JD002945.

——, A. Williams, H.-C. Huang, M. Caughey, and X.-Z. Liang, 2007: Sensitivity of U.S. surface ozone to future emissions and climate changes. *Geophys. Res. Lett.,* **34,** L08811, doi:10.1029/2007GL029455.

——, ——, ——, ——, and ——, 2008: Sensitivity of surface ozone simulation to cumulus parameterization. *J. Appl. Meteor. Climatol.,* **47,** 1456–1466.

Tie, X., and Coauthors, 2006: Chemical characterization of air pollution in Eastern China and the Eastern United States. *Atmos. Environ.,* **40,** 2607–2625.

Wang, H., L. Zhou, and X. Tang, 2006: Ozone concentrations in rural regions of the Yangtze Delta in China. *J. Atmos. Chem.,* **54,** 255–265, doi:10.1007/s10874-006-9024-z.

Washington, W. M., and Coauthors, 2000: Parallel climate model (PCM) control and transient simulations. *Climate Dyn.,* **16,** 755–774.

Wei, C.-F., and Coauthors, 2002: Seasonal variability of ozone mixing ratios and budgets in the tropical southern Pacific: A GCTM perspective. *J. Geophys. Res.,* **107,** 8235, doi:10.1029/2001JD000772.

Wesely, M. L., 1989: Parameterization of surface resistances to gaseous dry deposition in regional-scale numerical models. *Atmos. Environ.,* **23,** 1293–1304.

——, and B. B. Hicks, 2000: A review of the current status of knowledge on dry deposition. *Atmos. Environ.,* **34,** 2261–2282.

Wuebbles, D. J., K. O. Patten, M. T. Johnson, and R. Kotanarthi, 2001: New methodology for ozone depletion potentials of short-lived compounds: n-Propyl bromide as an example. *J. Geophys. Res.,* **106,** 14 551–14 572.

Yan, P., M. Wang, H. Cheng, and X.-J. Zhou, 2003: Distributions and variations of surface ozone in Changshu, Yangtze Delta region. *Acta Meteor. Sinica,* **17,** 205–217.

Zhang, L., J. Padro, and J. L. Walmsley, 1996: A multi-layer model vs single-layer models and observed O_3 dry deposition velocities. *Atmos. Environ.,* **30,** 339–345.